Table IV. Comparison of the Formation Constants[a] of Molybdate and Tungstate Complexes of Alditols

	erythro series			threo series		
	erythritol	galactitol	D-mannitol	DL-threitol	xylitol	D-glucitol
log K_W[b]	18.00	20.10	19.65	16.95	18.50	19.15
log K_{Mo}[c]	15.20	17.30	16.70	14.60	16.25	16.60
Δ	2.80	2.80	2.95	2.35	2.25	2.55

[a] Formation constant for the equilibrium (M = Mo or W, L = alditol) $2MO_4^{2-} + L + 2H^+ \rightleftarrows (2,1,2)^{2-} + H_2O$. Potentiometric values: *t*, 25 °C; *I* (KCl), 0.1 M. Δ is the difference log K_W − log K_{Mo}. [b] Reference 10. [c] Reference 14.

It prompted us to question the already mentioned remark[9] that the stabilities of tungstate and molybdate complexes of carbohydrates, including alditols, varied in parallel relationship (tungstate species are always more stable). For this purpose, we calculated the difference Δ between the logarithms of the formation constants, K_W or K_{Mo}, determined for the $(2,1,2)^{2-}$ complexes involving two tungstate or molybdate groups, one alditol, and two protons, using literature data[9,10,14] obtained in comparable conditions. That comparison (Table IV) showed that the claimed invariance of Δ was a rough approximation, as the Δ values could be separated into two groups corresponding to the erythro or threo series of alditols. Erythro ligands, including D-mannitol, were characterized by Δ values between 2.80 and 2.95. Comparable values, 3.00–3.15, were also reported for aldoses of lyxo-manno configuration.[9] Besides, threo compounds exhibited lower Δ values, typically 2.25 and 2.35. The higher value obtained for D-glucitol, Δ = 2.55, was probably biased by the side formation of minor ERY complexes and should be higher than the true difference between pure TH species. Thus, in the threo series, the stability enhancement due to the replacement of Mo by W is smaller than in the erythro series. It appears clearly that the existence of several structural series of complexes can explain the differences observed between the stabilities of molybdate and tungstate complexes of various alditols.

Conclusion

^{183}W NMR spectroscopy proved a powerful tool for the study of anionic tungstate complexes of carbohydrates in aqueous solution. Contrary to the ^{95}Mo NMR spectra, in which the resonances of both Mo atoms were confused in a single broad signal, ^{183}W NMR spectroscopy showed, for each dinuclear complex, two sharp signals coupled to protons via large long-range $^3J_{W,H}$ couplings, which allowed the estimation of the dihedral angles in the ERY type complexes. It demonstrated that their structures in solution were closely related to that reported in a X-ray study of the molybdate–erythritol complex.

On the other hand, we found that alditols of the threo species formed distinct types of complexes with molybdate (tetradentate) and tungstate (tridentate). The ^{183}W NMR signals were assigned to the structurally different W atoms (triply or doubly chelated) on the basis of comparison with the triply chelated atoms present in the erythro complexes.

Contribution from the Department of Chemistry,
Howard University, Washington, D.C. 20059

Mercury(II) Reactions with Water-Soluble Porphyrins

Louis R. Robinson and Peter Hambright*

Received August 26, 1991

Below pH 1 at 25 °C, equilibrium constants were measured for the reaction of Hg^{2+} with the free base of tetrakis(*N*-methyl-2-pyridiniumyl)porphyrin, the monocation of tetrakis(*N*-methyl-4-quinoliniumyl)porphyrin, and the diacid of tetrakis(*N*-methyl-4-pyridiniumyl)porphyrin, all of which produce complexes of the composition $Hg_2\text{–}P^{2+}$ which have the presumed structure $[Hg\text{–}P\text{–}Hg]^{2+}$. Near neutral pHs, the free bases of the pyridiniumylporphyrins form 1:1 adducts with mercury(II), formulated as $(HO)_2Hg\text{–}P^{2-}$ or $O\text{–}Hg\text{–}P^{2-}$, and the corresponding equilibrium constants are reported. Kinetic studies of the reaction of M(II) (M = Zn, Cu) with several of the Hg_2–Ps gave evidence for [M–P–Hg] intermediates, which either react with Hg^{2+} to re-form $Hg_2\text{–}P^{2+}$ or decompose to the final M(II)–P adduct. The catalysis of M(II)–P formation by added Hg(II) ions is traced to the extremely rapid formation of mercury–porphyrin intermediates.

Certain metal ions participate in labile equilibria with porphyrin molecules to form metalloporphyrins:

$$M^{2+} + H_2\text{–}P = M\text{–}P + 2H^+ \qquad (1)$$

Equilibrium constants for such 1:1 complexes have been measured in aqueous solutions for Zn(II),[1] Cd(II),[2] and Pb(II)[3] ions and in DMSO–water[4] mixtures for Zn(II) and Cu(II). Such Cd(II) and Pb(II) porphyrin intermediates[3,5] catalyze the incorporation of Zn(II), Co(II), Ni(II), and Mn(II) into porphyrins, where for example activated complexes of the composition [Zn–P–Cd] lead to Zn(II)–P production 10^2–10^3 times faster than the reaction of Zn(II) with H_2–P itself. The situation is rather more complicated for Ag(I)[6] and Hg(II) interactions with porphyrins. Along with Hg–P, Smith and co-workers have demonstrated in nonaqueous solution the existence of homodinuclear Hg–P–Hg species[7] and "double-sandwich" porphyrins[8] of the structure Hg–P–Hg–P–Hg. Adeyemo and Krishnamurthy[9] investigated certain of these re-

---

(1) Hambright, P. *Inorg. Chem.* **1977**, *16*, 2987.
(2) (a) Shamim, A.; Hambright, P. *Inorg. Chem.* **1980**, *19*, 564. (b) Shamim, A.; Hambright, P. *J. Inorg. Nucl. Chem.* **1979**, *42*, 1645.
(3) (a) Haye, S. E.; Hambright, P. *Inorg. Chem.* **1984**, *23*, 4777. (b) Tabata, M. *Analyst* **1987**, *112*, 141.
(4) Jimenez, H. R.; Julve, M.; Moratal, J. M.; Faus, J. *J. Chem. Soc., Chem. Comm.* **1987**, 910.
(5) Tabata, M.; Tanaka, M. *J. Chem. Soc., Dalton Trans.* **1983**, 1955.
(6) Okoh, J. M.; Bowles, N.; Krishnamurthy, M. *Polyhedron* **1984**, *3*, 1077.
(7) Hudson, M. F.; Smith, K. M. *Tetrahedron Lett.* **1974**, *26*, 2223.
(8) (a) Hudson, M. F.; Smith, K. M. *J. Chem. Soc., Chem. Commun.* **1973**, 515. (b) Hudson, M. F.; Smith, K. M. *Tetrahedron* **1975**, *31*, 3977. (c) Smith, K. M.; Eivazi, F. *J. Org. Chem.* **1979**, *44*, 2591.

0020-1669/92/1331-0652$03.00/0

Table I. Absorption Spectral Bands of Mercury (II) Porphyrins

porphyrin[a]	metal-free bands[b]	Hg_2–P^{2+} [c]	$(HO)_2$–Hg–P^{2-} [d]
H_2-TMPyP(2)	413 (2.3 × 10^5)	435.5 (2.0 × 10^5)	446 (1.7 × 10^5)
	512 (1.6 × 10^4)	564.5 (1.3 × 10^4)	580 (1.8 × 10^4)
	583 (5.2 × 10^3)	585.5 (sh)	
	634 (1.4 × 10^3)		
H_4-TMPyP(4)$^{2+}$	445 (2.5 × 10^5)	446.5 (2.0 × 10^5)	456 (1.8 × 10^5)
	591 (1.2 × 10^4)	565 (1.6 × 10^4)	584 (1.5 × 10^4)
	642 (1.6 × 10^4)		630 (1.0 × 10^4)
H_3-TMQP(4)$^+$	438 (1.0 × 10^5)	443.5 (1.5 × 10^5)	451 (9.8 × 10^4)
	576 (1.6 × 10^4)	560 (2.0 × 10^4)	580 (1.9 × 10^4)
	544 sh		
	623 (7.3 × 10^3)		

[a] Wavelengths are in nm and the extinction coefficients units are M^{-1} cm^{-1}. [b] H_2-TMPyP(x) data from ref 14b and the H_3-TMQP(4)$^+$ spectra from this work and ref 15. [c] Isosbestic points for the Hg^{2+} reactions: H_2-TMPyP(2), 426, 532, 622 nm; H_3-TMQP(4)$^+$, 451, 540, 567 nm; H_4-TMPyP(4)$^{2+}$, 452.5, 580.5 nm. [d] Isosbestic points for the $Hg(OH)_2$ reactions: H_2-TMPyP(2), 428, 487, 553, 623 nm; H_2-TMPyP(4), 440, 502, 562 nm; H_2-TMQP(4), 438.8, 505, 540 nm.

actions in water above pH 5. Tabata and Tanaka[10] have analytically determined low concentrations of mercury via the Hg(II) catalysis of Mn(III)–P formation and have also shown[11] that addition of Hg(II) to Zn^{2+}/H_4-P^{2+} mixtures allows a more rapid determination of Zn(II)–P (eq 1) formation constants.

Hg(II) is known to form Hg^{2+}, $Hg(OH)^+$, $Hg(OH)_3^-$, Hg_2OH^{3+}, $Hg_3(OH)_3^{3+}$, $Hg(OH)_2$, and $Hg(OH)^{3-}$ as a function of pH and mercury concentration.[12] We report the equilibrium constants of three differently protonated porphyrins with Hg(II) which produce Hg_2–P^{2+} in acid ranges where mercury is predominantly Hg^{2+} and the corresponding values for several free-base porphyrins with $Hg(OH)_2$ where mass law evidence indicates $(OH)_2Hg$–P^{2-} (or equivalently, O–Hg–P^{2-}) products near neutral pH. The kinetics of the reactions of dimercury porphyrins with Cu(II) and Zn(II) in acidic conditions give further insight into metal–porphyrin reactivity.

Experimental Section

The nitrate salts of the porphyrins tetrakis(N-methyl-4-pyridiniumyl)porphyrin [TMPyP(4)],[13] tetrakis(N-methyl-2-pyridiniumyl)porphyrin [TMPyP(2)],[14] and tetrakis(N-methyl-4-quinoliniumyl)porphyrin [TMQP(4)][15] were prepared by literature methods. Transition-metal nitrates were analyzed with edta, and the mercury(II) ions, by chloride titrations.[16] Absorption spectra were recorded on a Beckman DU 70 spectrophotometer, and all reactions were run at 25 ± 0.2 °C.

Results

Hg^{2+} and H_2-TMPyP(2). H_2-TMPyP(2) is monomeric in aqueous solution, and the pK_3 for the (H_2-P)(H^+)/(H_3-P^+) equilibria[2] is ∼−0.9. The tetrapositive charges due to the four pyridinium rings are not represented in this notation. This porphyrin is mainly in the H_2-P free-base form at H^+ concentrations below 0.9 M, and mercury(II) is predominately the Hg^{2+} ion below pH 1. The equilibrium constant for the formation of the dimercury complex (eq 2) of TMPyP(2) was studied at HNO_3 concentrations

$$2Hg^{2+} + H_2\text{-}P = Hg_2\text{-}P^{2+} + 2H^+ \quad K_{II} \tag{2}$$

from 0.13 to 0.86 M with an ionic strength I = 0.86 (HNO_3/$LiNO_3$). $Hg(NO_3)_2$ was varied from 9.6 × 10^{-4} to 1.9 × 10^{-2} M.

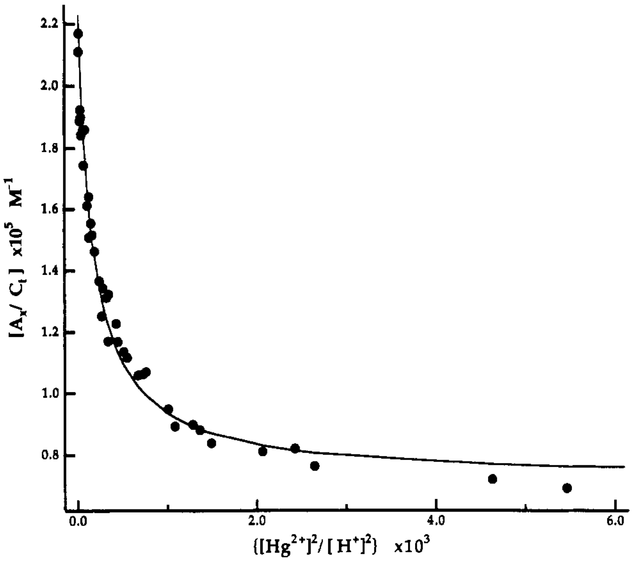

Figure 1. Plot of $[A_x/C_t]$ vs $[Hg^{2+}]^2/[H^+]^2$ for the reaction of Hg^{2+} with H_2-TMPyP(2) below pH 1.0. The dots are the experimental points, and the solid line is the theoretical curve calculated from eq 3.

In this pH range, the addition of Hg(II) leads to the very rapid disappearance of the H_2-TMPyP(2) bands (see Table I) and new peaks form due to Hg_2-P^{2+} at 435.5 and 564.5 nm. Isosbestic points are noted at 426, 532, and 622 nm. The equilibrium constant K_{II} was determined from the following equation:

$$A_x/C_t = [\epsilon_{H_2\text{-}P} + \epsilon_{Hg_2\text{-}P}(K_{II})(Hg^{2+})^2/(H^+)^2]/[(1 + K_{II}(Hg^{2+})^2)/(H^+)^2] \tag{3}$$

At constant wavelength, A_x is the observed absorbance, $\epsilon_{H_2\text{-}P}$ and $\epsilon_{Hg_2\text{-}P}$ are the extinction coefficients of the free base and dimercury porphyrins, C_t is the total porphyrin concentration, and K_{II} is the equilibrium constant of reaction 2. Equation 3 predicts that the ratio $[A_x/C_t]$ is constant for a constant Hg(II) and H^+ concentration. To prove this, H_2-TMPyP(2) was changed over an 85-fold range (9.7 × 10^{-8} to 8.2 × 10^{-6} M) at 2.0 × 10^{-2} M H^+ and 5.0 × 10^{-3} M Hg(II), and the observed ratios were found to vary by only ±2%. Figure 1 is a plot at 415.5 nm of $[A_x/C_t]$ vs $[(Hg^{2+})^2/(H^+)^2]$. Using a nonlinear least-squares program on eq 3 with $\epsilon_{H_2\text{-}P}$ as 2.3 × 10^5 M^{-1} cm^{-1}, we find K_{II} = (6.2 ± 0.4) × 10^3 and $\epsilon_{Hg_2\text{-}P}$ = (7.2 ± 0.2) × 10^4 M^{-1} cm^{-1}. The solid line in Figure 1 was calculated from these parameters, and there is excellent agreement (±0.03 absorbance units) between the experimental and calculated values, for each of the 39 points studied.

Hg(II) and H_4-TMPyP(4)$^{2+}$. TMPyP(4) can exist[17] as the free-base H_2-P, as well as the mono and dications H_3-P^+ and H_4-P^{2+} below pH 7. At an ionic strength of 1.9 ($LiNO_3$/HNO_3), we determined by standard methods[17,18] that pK_3 = 3.0 ± 0.1 and pK_4 = 2.2 ± 0.1, where K_4 is for the (H_3-P^+)(H^+)/(H_4-P^{2+}) equilibria. The reaction of Hg^{2+} with the diacid H_4-TMPyP(4)$^{2+}$ was studied from 0.2 to 0.7 M in H^+, using Hg(II) concentrations from 2.6 × 10^{-2} to 2.1 × 10^{-1} M. The process was found to be

$$2Hg^{2+} + H_4\text{-}P^{2+} = Hg_2\text{-}P^{2+} + 4H^+ \quad K_{IV} \tag{4}$$

The reactions were monitored at 640 nm, where A_0 and A_∞ are the absorbancies of solutions fully in the H_4-P^{2+} and Hg_2-P^{2+} forms, respectively, while A_x are those of mixtures of the two species. It is readily shown that

$$(A_0 - A_x)^{-1} = K_{IV}(A_0 - A_\infty)^{-1}\{[Hg^{2+}]^2/[H^+]^4\} + (A_0 - A_\infty)^{-1} \tag{5}$$

Figure 2 is a linear plot of $(A_0 - A_x)^{-1}$ vs $[Hg^{2+}]^2/[H^+]^4$, from which the equilibrium constant K_{IV} = (2.4 ± 0.1) × 10^{-1} M^2 was determined. The Hg_2–TMPyP(4)$^{2+}$ peak positions and related

---

(9) (a) Adeyemo, A.; Krishnamurthy, M. *Inorg. Chim. Acta* **1984**, *83*, L41. (b) Adeyemo, A.; Krishnamurthy, M. *Inorg. Chem.* **1977**, *16*, 3355.

(10) Tabata, M.; Tanaka, M. *Anal. Lett.* **1980**, *13*, 427.

(11) Tabata, M.; Tanaka, M. *J. Chem. Soc., Chem. Commun.* **1985**, 42.

(12) Bases, C.; Mesmer, R. E. *The Hydrolysis of Cations*; Robert E. Krieger Publishing Co.: Malabar, FL, 1986.

(13) Hambright, P.; Fleischer, E. B. *Inorg. Chem.* **1970**, *9*, 1757.

(14) (a) Hambright, P.; Gore, T.; Burton, M. *Inorg. Chem.* **1976**, *15*, 2314. (b) Kalyanasundaram, K. *Inorg. Chem.* **1984**, *23*, 2453.

(15) Adeyemo, A.; Shamim, A.; Hambright, P.; Williams, R. F. X. *Ind. J. Chem.* **1982**, *21A*, 763.

(16) Vogel, A. *Vogel's Textbook of Quantitative Inorganic Analysis Including Elementary Instrumental Analysis*; Bassett, J., Denny, R. C., Jeffrey, G. H., Mendham, J., Eds.; Longman Scientific & Technical: Essex, England, 1978.

(17) Baker, H.; Hambright, P.; Wagner, L. *J. Am. Chem. Soc.* **1973**, *95*, 5942.

(18) Pasternack, R.; Sutin, N.; Turner, D. *J. Am. Chem. Soc.* **1976**, *98*, 1908.

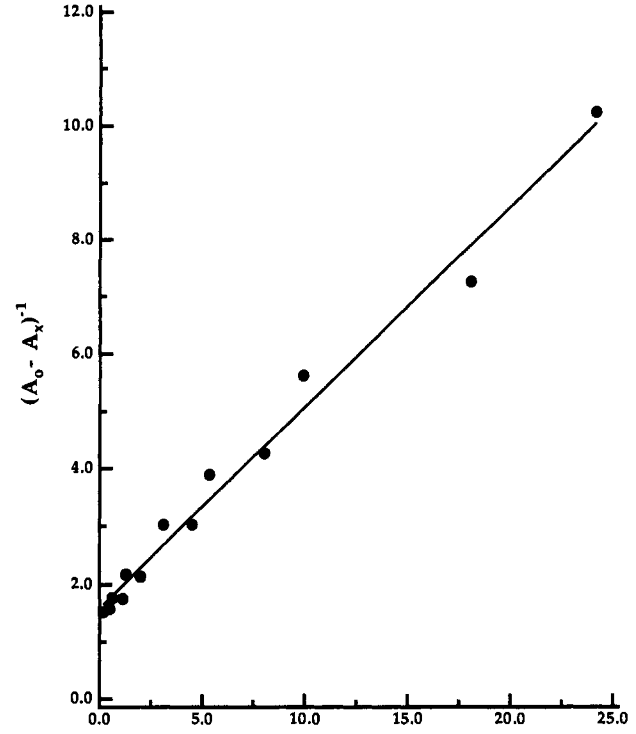

Figure 2. Plot of $(A_0 - A_x)^{-1}$ vs $\{[Hg^{2+}]^2/[H^+]^4\}$ for the Hg^{2+}/H_4-TMPyP$(4)^{2+}$ reaction (eq 5).

Table II. pK_a and Formation Constants for Mercury(II) with Porphyrins[a]

	H_2-TMPyP(2)	H_2-TMQP(4)	H_2-TMPyP(4)
pk_3[b]	−0.9	1.0 ± 0.1	3.0 ± 0.1
pK_4			2.2 ± 0.1
		Hg_2–P^{2+}	
K_{II}	(6.2 ± 0.4) × 10^3	(5.6 ± 1.6) × 10^3	(3.8 ± 2.1) × 10^4
K_{III}		(5.6 ± 1.0) × 10^2	(3.8 ± 1.8) × 10
K_{IV}			(2.4 ± 0.1) × 10^{-1}
		$(HO)_2Hg$–P^{2-}	
K_I	(3.5 ± 0.2) × 10^{-5}		(2.3 ± 0.1) × 10^{-6}

[a] The italic equilibrium constants were experimentally determined. [b] The pK_as were measured at the same ionic strength as the corresponding equilibrium constant (see text), while K_I was studied at I = 0.1.

isosbestic points are in Table I.

Hg(II) and H_3-TMQP(4)$^+$. In contrast to TMPyP(4)[17] and TMQP(3),[15] TMQP(4) forms only H_2-P and H_3-P^+ up to 2.0 M acid concentrations. A pK_3 of 1.0 ± 0.1 was determined at I = 1.9. The reaction between Hg^{2+} and H_3-TMQP(4)$^+$ was studied between 0.80 and 1.3 M H^+ at I = 1.9, with $[Hg^{2+}]$ from 5.0 × 10^{-2} to 4.2 × 10^{-1} M. Using data analysis techniques as outlined above for TMPyP(4), K_{III} for TMQP(4) (eq 6) was found to be (5.6 ± 1.0) × 10^2 M (Table II).

$$2Hg^{2+} + H_3\text{-}P^+ = Hg_2\text{–}P^{2+} + 3H^+ \quad K_{III} \tag{6}$$

$Hg(OH)_2$ and H_2-TMPyP(2, 4). Mercury(II) is mainly[12] $Hg(OH)_2$(aq) from pH 4 to 10. In order to determine the nature of the reactions of H_2-P with mercury in this pH range, we noted that the spectra of solutions containing roughly equal amounts of mercury to porphyrin became independent of pH above pH 6. At I = 0.1 ($LiNO_3$), with 2.0 × 10^{-3} M HEPES (4-(2-hydroxyethyl)-1-piperazineethanesulfonic acid) as the buffer, a constant H_2-TMPyP(4) concentration of 6.5 × 10^{-6} M was titrated at pH 7.5 with varying amounts of mercury(II) from 1.2 × 10^{-6} to 1.6 × 10^{-5} M. Equilibrium was rapidly attained, and Figure 3 shows a plot of the absorbance at 456 nm verses the ratio ([Hg]/[H_2-P]). The sharp break at the 1:1 ratio is interpreted as one mercury reacting with one H_2-TMPyP(4), and the same behavior was shown for mercury with H_2-TMPyP(2). By variation of the mercury concentrations in the pH range 7.5–4, the reaction that took place was found to be

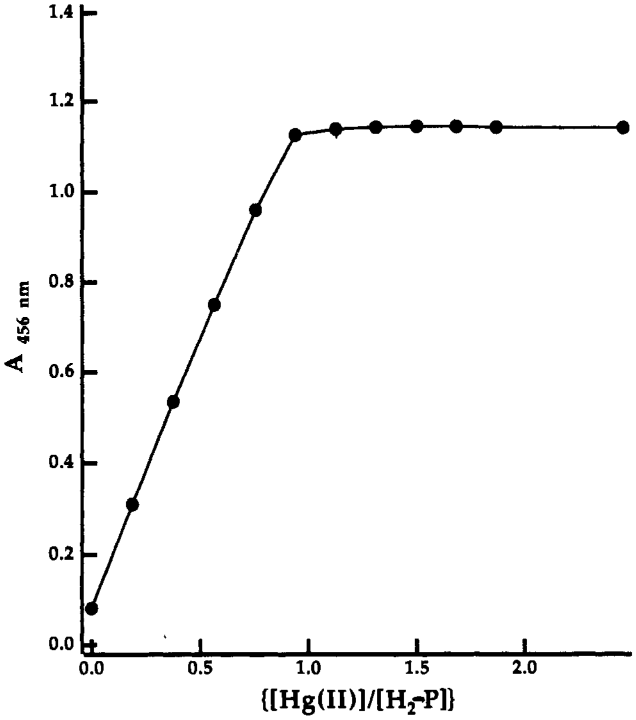

Figure 3. Plot of A_{456} nm vs {[Hg(II)]/[H_2-P]}, indicating the 1:1 complex formed between $Hg(OH)_2$ and H_2-TMPyP(4) at pH 7.5.

Table III. Kinetic Data for the M^{2+}/Hg_2–P^{2+} Exchange Reactions

reacn	k_1, M^{-1} s^{-1}	k_{-1}/k_2, M^{-1}
Cu^{2+}/Hg_2–TMPyP$(2)^{2+}$	4.3 ± 0.7	(8.4 ± 1.4) × 10^2
Zn^{2+}/Hg_2–TMPyP$(2)^{2+}$	(7.1 ± 2.6) × 10	(4.6 ± 2.0) × 10^3
Cu^{2+}/Hg_2–TMPyP$(4)^{2+}$	5.2 ± 3.2	(2.1 ± 0.6) × 10^2
Cu^{2+}/Hg_2–TMQP$(4)^{2+}$	1.6 ± 0.2	(4.3 ± 0.5) × 10^2

$$Hg(OH)_2 + H_2\text{-}P = (OH)_2Hg\text{–}P^{2-} + 2H^+ \quad K_I \tag{7}$$

Isosbestic points were noted throughout the course of the titration (Table I), and K_I for H_2-TMPyP(4) was (2.3 ± 0.1) × 10^{-6} M. Similar isosbestic behavior occurred in the formation of $(OH)_2Hg$–TMPyP$(2)^{2-}$ (which is equivalent to O–Hg–TMPyP-$(2)^{2-}$), where K_I = (3.5 ± 0.2) × 10^{-5} M.

Kinetics of Cu^{2+} and Hg_2-TMPyP$(2, 4)^{2+}$. Below pH 1, addition of excess Cu^{2+} to Hg_2–TMPyP$(2)^{2+}$ solutions led ultimately to complete formation of Cu(II)–TMPyP(2), with its characteristic peaks at 416.5 and 550 nm. Isosbestic points occurred at 426, 470, 521, 555, 574, and 584 nm during the course of the reaction, indicating that Cu–P and Hg_2–P^{2+} were the major absorbing species. These kinetics were followed at 416.5 nm at differing concentrations of Hg^{2+} (9.7 × 10^{-4} to 1.5 × 10^{-2} M), Cu^{2+} (5.2 × 10^{-4} to 1.6 × 10^{-2} M), and H^+ (1.3 × 10^{-1} to 8.6 × 10^{-1} M), with the ionic strength 0.86. The reactions were first order in porphyrin over 3 half-lives, first order in Cu^{2+}, and of an indefinite order in Hg^{2+} in the ranges investigated. The proposed mechanism is

$$Cu^{2+} + Hg_2\text{–}P^{2+} = [Cu\text{–}P\text{–}Hg]^{2+} + Hg^{2+} \quad k_1, k_{-1} \tag{8}$$

$$[Cu\text{–}P\text{–}Hg]^{2+} \rightarrow Cu\text{–}P + Hg^{2+} \quad k_2 \tag{9}$$

With $[Cu\text{–}P\text{–}Hg]^{2+}$ as a steady-state intermediate, the observed pseudo-first-order rate constant is of the form

$$k_{obsd} = \{(k_1k_2[Cu^{2+}]Q)/(k_{-1}[Hg^{2+}] + k_2)\} \tag{10}$$

where $Q = K_{II}[Hg^{2+}]^2/(K_{II}[Hg^{2+}]^2 + [H^+]^2)$. Figure 4 shows a linear plot of $([Cu^{2+}]Q/k_{obsd})$ vs $[Hg^{2+}]$. On the basis of eq 10, k_1 and the ratio (k_{-1}/k_2) for TMPyP(2) are reported in Table

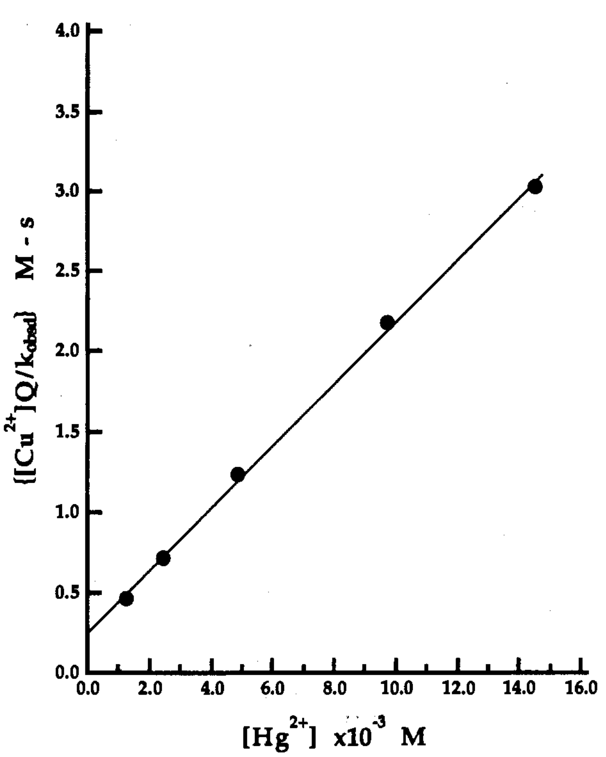

Figure 4. Plot of {[Cu^{2+}]Q/k_{obsd}} vs [Hg^{2+}] for the Cu^{2+}/Hg$_2$–TMPyP(2)$^{2+}$ reaction (eq 10).

III for both Cu^{2+} and Zn^{2+} as entering ions. The dimercury TMPyP(4) and TMQP(4) porphyrins also followed the same mechanism with Cu^{2+}, where the form of Q was modified to reflect the appropriate order in proton concentration.

Kinetics of the Zn(II)/(OH)$_2$Hg-TMPyP(4)$^{2-}$ Reaction. The kinetics of the displacement of Hg from (OH)$_2$Hg–TMPyP(4)$^{2-}$ by Zn(II) was studied at pH 5.6, I = 0.12 (LiNO$_3$), with 10^{-3} M MES (4-morpholineethanesulfonic acid) as the buffer. H$_2$-TMPyP(4) was completely converted into the mercury porphyrin with 5 × 10^{-3} M Hg(II), and the unidirectional formation of Zn(II)–TMPyP(4) was first order in porphyrin and Zn(II) concentration (2.0 × 10^{-5} to 4.0 × 10^{-4} M), with a specific rate constant of (5.9 ± 0.3) × 10^1 M^{-1} s^{-1}. Under the same conditions, the Zn(II)/H$_2$-TMPyP(4) reaction was first order in each component, with k_{obsd}/[Zn(II)] = (4.1 ± 0.3) × 10^{-1} M^{-1} s^{-1}.

Discussion

The pK_{a_1} of Hg^{2+} is ~3.7, and below pH 1, the Hg^{2+} ion predominates.[12] Our results indicate that the differently protonated forms of the three water-soluble positively charged porphyrins, H$_2$-TMPyP(2), H$_3$-TMQP(4)$^+$, and H$_4$-TMPyP(4)$^{2+}$, react rapidly with Hg^{2+} in acid to form Hg$_2$–P^{2+}. At millimolar Hg^{2+} and micromolar H$_2$-TMPyP(2) levels, the reactions are too fast to be followed by stopped-flow techniques. From work in dmf solutions, the incorporation rate ratio $k_{Hg(II)}/k_{Zn(II)}$ for M(II)–P formation is ~10^7 for tetraphenylporphyrin (TPP)[19] and ~10^5 for N-methyltetraphenylporphyrin,[20] while near neutral pH in water with the tetrakis(4-N,N,N-trimethylaniliniumyl)porphyrin (TAPP)[21] the ratio is ~10^3. In contrast to the other first-row divalent transition-metal ions, the larger size (0.69, 0.92, and 0.93 Å for divalent Zn, Cd, and Hg), lower coordination number, and higher solvent lability ($k_{Hg(II)}/k_{Zn(II)}$ for dmf exchange is ~10^2) of Hg(II) may partially explain its much enhanced reactivity with porphyrins. Since the pK_3 and pK_4 porphyrin protonation constants are known, K_{II} values for the three porphyrins in their H$_2$-P forms reacting with Hg^{2+} are readily calculated. As shown in Table II, the K_{II}s for the three compounds are of the same order of magnitude and average ~10^4. In a footnote mentioning results at unspecified acidities, Tabata and Tanaka[11] report a K_{IV} of 5.6 × 10^{-6} M^2 for Hg$_2$–TPPS^{2+} (tetrakis(4-sulfonatophenyl)porphyrin), with a K_{II} of ~3 × 10^5.

On the basis of NMR spectroscopy, Hudson and Smith[8] assigned a (H$_2$O(oAc)–Hg–P–Hg(oAc)(H$_2$O) structure to their dinuclear Hg$_2$–TPP^{2+} complex, with the mercury ions on opposite sides of the porphyrin plane. The same is postulated for the Hg$_2$–Ps found in this study, with the general formula [(OH$_2$)$_2$Hg–P–Hg(OH$_2$)$_2$]$^{2+}$. The mercury ions could be tetrahedrally hybridized, with each Hg bonded to the two opposite nitrogen atoms of the porphyrin core. The M^{2+}/Hg$_2$–P^{2+} kinetics indicate the existence of a [Hg–P–M] intermediate, where, by analogy, the M and Hg are on opposite sides of the porphyrin plane. In the Zn^{2+}/Cd–P and related exchange reactions,[2,3,5] the rate law is first order in each component and this leads to the postulation of either opposite [Zn–P–Cd] or same side [M–Zn–P] transition-state structures. The M^{2+}/Hg$_2$–P^{2+} results thus lend weight to the opposite side formulations in such heteronuclear metal-exchange reactions.

The rate law for the Cu^{2+}/H$_2$-TMPyP(2) process is first order in each reactant, with a specific rate constant of 2.9 × 10^{-3} M^{-1} s^{-1}, and since k_1 = 4.3 M^{-1} s^{-1} for Cu^{2+}/Hg$_2$–TMPyP(2), the Cu^{2+} reacts ~10^3 times faster with this dimercury porphyrin than the free base. It must be noted that the reactivity of TMPyP(2) is usually different from that found for most other water-soluble porphyrins and could be a reflection of the ortho N-methyl groups hindering porphyrin nucleus deformation,[19,22] which results in lower proton basicities and decreased metal incorporation rates. Similar reactivity comparisons are more tenuous with the more basic and more reactive TMPyP(4) and TMQP(4) complexes, which lack ortho substituents. For these compounds, the variety of unreactive protonated species in solution has led to studies under widely different ionic strength and pH conditions.[23] Nevertheless, it appears that there is no large difference in rate constants between the M(II)/Hg$_2$–P k_1s and corresponding values for metal incorporation into H$_2$-P.

With typical M^{2+}/H$_2$-P systems,[24] the order of specific rate constants in the acid range is usually Cu > Zn > Mn > Ni, while for M^{2+}/Hg$_2$–TMPyP(2), we qualitatively find below pH 1 Zn > Cu ~ Mn ≫ Ni. This reversal may reflect the preference for tetrahedral as opposed to octahedral coordination geometries during the formation of the transition state. In 0.4 M HNO$_3$, 10 mM Hg^{2+} does not displace Cu from preformed 10 μM Cu(II)–TMPyP(4) after 48-h standing, and all of the Cu^{2+}/Hg$_2$–P reactions went to completion. The ratio (k_{-1}/k_2) is a reflection of Hg^{2+} displacing M from the [Hg–P–M] intermediate to re-form the [Hg–P–Hg] reactant, and the ratio is ~10^2 for Cu and Zn. This might indicate that M is weakly bonded and two coordinate with respect to the porphyrin in the intermediate and four coordinate and tightly bound in the M(II)–P product. This increase in the coordination number of M is part of the driving force of the M^{2+}/Hg$_2$–P reactions.

In neutral solutions, the mole ratio and mass law studies indicate the production of (OH)$_2$Hg–P^{2-}, which can also be formulated as O–Hg–P^{2-}. From measurements at a single pH in the neutral region, Adeyemo and Krishnamurthy[9a] also found spectral evidence for 1:1 complexes with low concentrations of TAPP and TPPS. The (OH)$_2$Hg–TMPyP(4)$^{2-}$ reacts ~140 times faster than Zn(II) than does H$_2$-TMPyP(4) and thus behaves like the Cd(II)–P and Pb(II)–P counterparts, where the metals are substantially above the mean porphyrin plane. In the TAPP system,[21] Hg(II) enhances the zinc(II) incorporation rate by factor of 5 × 10^3. The catalysis of Mn(II)–TPPS (tetrakis(4-sulfonatophenyl)porphyrin) formation[25] is in the order Hg(II) ≫ Cd(II)

---

[19] Robinson, L. R.; Hambright, P. *Inorg. Chim. Acta* **1991**, *185*, 17.

[20] Funahashi, S.; Yamaguchi, Y.; Tanaka, M. *Inorg. Chem.* **1984**, *23*, 2249.

[21] (a) Adeyemo, A.; Krishnamurthy, M. *Int. J. Chem. Kinet.* **1984**, *16*, 1075. (b) Thompson, A. N.; Krishnamurthy, M. *J. Inorg. Nucl. Chem.* **1979**, *41*, 1251.

[22] Mosseri, M.; Nahor, G. S.; Neta, P.; Hambright, P. *J. Chem. Soc., Faraday Trans.* **1991**, *87*, 2567.

[23] Nwaeme, J.; Hambright, P. *Inorg. Chem.* **1984**, *23*, 1990.

[24] Lavallee, D. K. *Coord. Chem. Rev.* **1985**, *61*, 55.

[25] Tabata, M.; Tanaka, M. *Inorg. Chim. Acta Lett.* **1980**, *40*, X71.

Table IV. Equilibrium Constants[a] for 1:1 Complexes of Metal Ions with Free-Base Porphyrins

	TMPyP(2) pK_3 −0.9	TMPyP(4) pK_3 1.4	TAPP pK_3 3.6	TPPS pK_3 4.8
Zn(II)[b]	1.9×10^{2}	4.4	1.1	1.3×10^{-1}
$Hg(OH)_2$[c]	3.5×10^{-5}	2.3×10^{-6}	5.0×10^{-9}	4.0×10^{-9}
Cd(II)[d]	7.9×10^{-7}	6.1×10^{-9}	1.7×10^{-10}	8.3×10^{-11}
Pb(II)[e]	9.5×10^{-8}	2.0×10^{-8}	3.0×10^{-10}	3.4×10^{-10}

[a] Equilibrium constant (eq 1) units are M, at 25 °C. [b] TMPyP(2, 4), ref 1; TAPP, ref 21b; TPPS, ref 11. [c] TMPyP(2, 4), this work; TAPP and TPPS, ref 9a. [d] TPPS, ref 5, other porphyrins, ref 2. [e] TPPS, ref 3b; other porphyrins, ref 3a.

> Pb(II). This is because $(HO)_2Hg{-}P^{2-}$ forms orders of magnitude faster than the Pb or Cd(II)–P intermediates. Once formed, the rate constants for the reactions of any of these intermediates with a given entering ion are not vastly different. For example, the specific rate constants for Zn^{2+} incorporation into $(OH)_2$–Hg, Cd(II), and Pb(II)–TMPyP(4) are ~56, 79, and 14 M^{-1} s^{-1}, respectively.[3]

The $Zn^{2+}/H_4\text{-}TPPS^{2+}$ reactions come to equilibrium very slowly at pH 3.5, and Tabata and Tanaka demonstrated that the addition of 2.1×10^{-5} M Hg(II) leads to a more rapid determination of K_{IV} for this system, presumably via the formation of reactive mercury–porphyrin intermediates.[26] We noted with $H_4\text{-}TPPS^{2+}$ at this pH, however, that Hg(II) levels above ~10^{-4} M lead to rapid decomposition of this porphyrin into unknown species. These products could involve the substitution of the TPPS β-pyrrole protons by Hg atoms, a process found by Smith and co-workers[27] to occur in the highly basic deuteroporphyrin type series. The experiments reported in this paper were done with positively charged porphyrins which are substantially less basic than TPPS, and no changes in porphyrin spectra that could be attributed to the alteration in the β-pyrrole positions were ever found at any Hg(II) levels studied over the several hours that it took to collect our results. However, with micromolar levels of Cu(II)–TMPyP(4) in ~0.4 M HNO_3 and 0.1–0.5 M Hg(II), both the visible and Soret bands gradually shift over a period of days to higher wavelengths, consistent with the slow substitution of several β-pyrrole protons by Hg(II).

Table IV shows a comparison of the formation equilibrium constants that have been measured for 1:1 metal/porphyrin complexation. In general, the order is Zn(II) ≫ Hg(II) > Cd(II) ~ Pb(II). For a given metal ion, less basic porphyrins have larger formation constants. As noted previously,[2] this is due to the fact that the reverse $[H^+/M(II){-}P]$ rate constants depend more strongly on porphyrin basicity than do the magnitudes of the forward $[M^{2+}/H_2\text{-}P]$ specific rates.

In conclusion, equilibrium constants have been measured below pH 1 for Hg^{2+} and various H_2-P, H_3-P^+, and H_4-P^{2+} porphyrins which all produce the homodinuclear $[Hg_2{-}P]^{2+}$ as a product. The reactant in each case is probably the free base, since most metal ions in aqueous solution are less reactive with the protonated mono- or dication porphyrins.[17,24] Near neutral pH, $Hg(OH)_2$ and H_2-P form $(OH)_2Hg{-}P^{2-}$ (or O–Hg–P^{2-}) mononuclear adducts. The overall pattern is similar to that observed by Hudson and Smith[28] in their spectral study of Hg(II)–TPP. In methylene chloride Hg(II)–TPP is stable, and added traces of acid convert 2 Hg(II)–P into H_2-P and Hg_2–P^{2+}. Hg_2–P^{2+} then reacts with additional protons to form H_2-P and Hg^{2+}. This is in agreement with our results indicating that Hg_2–P^{2+} is more stable than Hg(II)–P under acidic conditions.

Registry No. TMPyP(4), 38673-65-3; TMPyP(2), 59728-89-1; TMQP(4), 85254-98-4; Hg, 7439-97-6; Cu, 7440-50-8; Zn, 7440-66-6.

---

(26) At 0.70 M H^+, $I = 0.86$, with 5.0×10^{-4} M added Hg^{2+}, we found a formation constant for Zn(II)–TMPyP(2) of $(2.4 \pm 0.1) \times 10^{2}$ M, as compared to the uncatalyzed value of 1.9×10^{2} M measured earlier[1] under slightly different conditions.

(27) (a) Smith, K. M.; Langry, K. C. *J. Org. Chem.* **1983**, *48*, 500. (b) Smith, K. M.; Langry, K. C.; Minnetian, O. M. *J. Org. Chem.* **1984**, *49*, 4609.

(28) Hudson, M. F.; Smith, K. M. *Tetrahedron Lett.* **1974**, *26*, 2227.

Contribution from the Department of Chemistry,
University of Victoria, P.O. Box 3055, Victoria, BC, Canada V8W 3P6

Thermo- and Photoaquation of *trans*-$[Cr(1,3\text{-diaminopropane})_2(CN)_2]ClO_4$. Quenching of Photochemistry by Photoproducts

Alexander David Kirk* and S. Rupasiri L. Fernando

Received April 25, 1991

The compound *trans*-$[Cr(tn)_2(CN)_2]ClO_4$, where tn = 1,3-diaminopropane, has been prepared and characterized. It undergoes an acid-catalyzed thermal aquation of the cyanide ligand to yield *trans*-$Cr(tn)_2(H_2O)(CN)^{2+}$ with a pseudo-first-order rate constant of 8×10^{-6} s^{-1} at 5×10^{-4} M H^+ and 15 °C. The further aquation to yield *trans*-$Cr(tn)_2(H_2O)_2^{3+}$ is significantly slower, so that solutions of relatively pure *trans*-$Cr(tn)_2(H_2O)(CN)^{2+}$ can be prepared by this route. Under these conditions, no aquation of the Cr–tn bond is observed. Photoaquation of *trans*-$[Cr(tn)_2(CN)_2]ClO_4$ was examined by difference spectroscopy, reversed-phase liquid chromatography, and direct proton uptake and cyanide release measurements. Both cyanide and tn are aquated. The proton uptake measurements showed that the photolysis behavior is nonlinear owing to quenching of the photoreactant doublet state by photoproducts. The total product quantum yields were therefore based on the zero-time slopes of the proton uptake data. $\phi(CN^-)$, $\phi(tnH^+)$ (irradiation wavelength): 0.035 ± 0.004, 0.048 ± 0.005 (436 nm); 0.023 ± 0.004, 0.052 ± 0.004 (458 nm). Loss of cyanide is not predicted by photochemical theory, and its occurrence is attributed to the role of ligand interactions in directing photoaquation modes.

Introduction

Zinato, Riccieri, and co-workers have reported[1-9] the thermal aquation and photoaquation behavior of an interesting series of cyano ammine complexes. Some of these molecules have long-lived doublet states which emit from room-temperature aqueous solutions, offering a favorable circumstance for the study of photophysical behavior of the excited states under photochemical conditions.

The dynamics of Cr(III) photochemistry has been elucidated by studies on the wavelength and temperature dependence of

---

* To whom correspondence should be addressed.

(1) Riccieri, P.; Zinato, E. *Inorg. Chem.* **1980**, *19*, 853.
(2) Riccieri, P.; Zinato, E. *Inorg. Chem.* **1980**, *19*, 3279.
(3) Zinato, E.; Riccieri, P.; Prelati, M. *Inorg. Chem.* **1981**, *20*, 1432.
(4) Riccieri, P.; Zinato, E. *Inorg. Chem.* **1981**, *20*, 3722.
(5) Riccieri, P.; Zinato, E. *Inorg. Chem.* **1983**, *22*, 2305.
(6) Zinato, E.; Adamson, A. W.; Reed, J. L.; Puaux, J. P.; Riccieri, P. *Inorg. Chem.* **1984**, *23*, 1138.
(7) Riccieri, P.; Zinato, E. *Inorg. Chem.* **1985**, *24*, 441.
(8) Zinato, E.; Adamson, A. W.; Riccieri, P. *J. Phys. Chem.* **1985**, *89*, 839.

0020-1669/92/1331-0656$03.00/0 © 1992 American Chemical Society